Proceedings of "Applications of Physics in Mechanical and Material Engineering" (APMME 2023)

Numerical Evaluation of the Impact of Selected Physical Phenomena and Riser Shape on the Formation of Shrinkage Defects in the Casting–Riser System

L. Sowa* and T. Skrzypczak

Department of Mechanics and Machine Design Fundamentals, Faculty of Mechanical Engineering and Computer Science, Czestochowa University of Technology, Dąbrowskiego 73, 42-201 Częstochowa, Poland

Doi: 10.12693/APhysPolA.144.296 *e-mail: leszek.sowa@pcz.pl

Understanding the complex physical phenomena involved in the casting process simulation requires continuous and complementary research to improve mathematical modelling. The paper presents a mathematical model and numerical simulations of the solidification process of a cylindrical casting, taking into account the filling of the mould cavity with liquid metal and feeding the casting through the riser during solidification. The basic mathematical model that considers only thermal phenomena is often insufficient to analyse the metal solidification process. Therefore, more complex models are formulated that include coupled thermal and flow phenomena. The mathematical description then consists of the system of Navier–Stokes differential equations, the equations of the continuity of flow and energy. Such a mathematical model was used in the paper because the mutual dependence of thermal and flow phenomena has a significant impact on the solidification process. The finite element method was used to solve the problem, and changes in thermophysical parameters were considered as a function of temperature. The impact of the riser shape on the effectiveness of feeding of the solidifying casting was also determined and an appropriate selection of the riser shape was made to obtain a casting without shrinkage defects, which was the aim of this work.

topics: numerical simulations, solidification, Navier–Stokes equations, casting defect

1. Introduction

During the casting process, various types of defects occur that may have a negative impact on the quality of the final product. One of such defects is the formation of shrinkage cavities, which cannot be completely avoided, but the heat transport process can be controlled so as to reduce these defects by moving their location to the riser. Research on real objects is much more difficult, which is why computer simulations are becoming the basic method of controlling the casting solidification process [1–7]. In this paper, the course of the solidification process is analysed in the cylindrical or conical-shaped casting–riser system using a basic or complex model. In the complex model [2, 3, 5, 6], the mutual influence of thermal and flow phenomena was taken into account, starting from the moment of filling the metal mould with molten metal and ending with complete solidification of the casting. For comparison, the solidification process of the casting was analysed using the basic model [4], in which only thermal phenomena are taken into account. In this way, the impact of taking into account or omitting liquid metal movements on the process of making a casting without shrinkage defects was assessed, which was the purpose of this paper. The shape of the solidus line was also observed, assessing whether it was closed in the casting area. Such a situation would mean no inflow of molten metal from the riser to this area in the casting and the formation of a shrinkage defect in this place of the casting, which we try to avoid.

2. The mathematical model

The mathematical model of the casting solidification process considering the liquid metal movements (complex model) is based on the solution of the following system of equations in a cylindrical axial-symmetric coordinate system [2–7]:

- Navier–Stokes equations

$$\mu\left(\frac{\partial^2 v_r}{\partial r^2}+\frac{1}{r}\frac{\partial v_r}{\partial r}+\frac{\partial^2 v_r}{\partial z^2}-\frac{v_r}{r^2}\right)-\frac{\partial p}{\partial r}+\rho g_r$$
$$+\rho g_r\beta\,(T-T_\infty)_r=\rho\frac{\mathrm{d}v_r}{\mathrm{d}t},$$
$$\mu\left(\frac{\partial^2 v_z}{\partial r^2}+\frac{1}{r}\frac{\partial v_z}{\partial r}+\frac{\partial^2 v_z}{\partial z^2}\right)-\frac{\partial p}{\partial z}+\rho g_z$$
$$+\rho g_z\beta\,(T-T_\infty)=\rho\frac{\mathrm{d}v_z}{\mathrm{d}t}, \tag{1}$$

- continuity equation

$$\frac{\partial v_r}{\partial r}+\frac{v_r}{r}+\frac{\partial v_z}{\partial z}=0, \tag{2}$$

- heat conductivity equation with the convection term

$$\lambda\frac{\partial T}{\partial r}+\frac{\partial}{\partial r}\left(\lambda\frac{\partial T}{\partial r}\right)+\frac{\partial}{\partial z}\left(\lambda\frac{\partial T}{\partial z}\right)=$$
$$\rho C_{ef}\frac{\partial T}{\partial t}+\rho C_{ef}\left(v_r\frac{\partial T}{\partial r}+v_z\frac{\partial T}{\partial z}\right), \tag{3}$$

- first order pure advection equation

$$\frac{\partial F}{\partial t}+v_r\frac{\partial F}{\partial r}+v_z\frac{\partial F}{\partial z}=0, \tag{4}$$

where λ is thermal conductivity coefficient [W/(m K)]; $\mu(T)$ — dynamical viscosity coefficient [kg/(m s)]; ρ=$\rho(T)$ — density [kg/m^3]; v_r and v_z — the r- and z-component of velocity [m/s], respectively; T — temperature [K]; C_{ef} = c+$L/(T_L-T_S)$ — effective specific heat of a mushy zone [J/(kg K)]; L — latent heat of solidification [J/kg]; T_L and T_S — the liquidus and solidus temperature of the analysed alloy, [K]; g_r and g_z — the r- and z-component of gravitational acceleration [m/s^2], respectively; p — pressure [N/m^2]; β — volume coefficient of thermal expansion [1/K]; t — time [s]; c — specific heat [J/(kg K)]; r — radius [m]; T_∞ — reference temperature (T_∞=T_{in}) [K]; F — the pseudo-concentration function across the elements lying on the free surface.

The mathematical model of the casting solidification process without taking into account the movements of liquid metal (basic model) is reduced only to the solution of the heat conductivity equation (3) without the convection term [4].

The equations (1)–(4) are completed by appropriate boundary conditions and initial conditions. The initial conditions for temperature and velocity fields are given, respectively, as [3–5]

$$\boldsymbol{v}(r,z,t_0)=\boldsymbol{v}_0(r,z)=v_{in}\Big|_{\Gamma_{1-1}},$$

$$T(r,z,t_0)=T_0(r,z)=\begin{cases}T_{in} & \text{on } \Gamma_{1-1}\\ T_A & \text{in } \Omega_A\\ T_M & \text{in } \Omega_M\end{cases}. \tag{5}$$

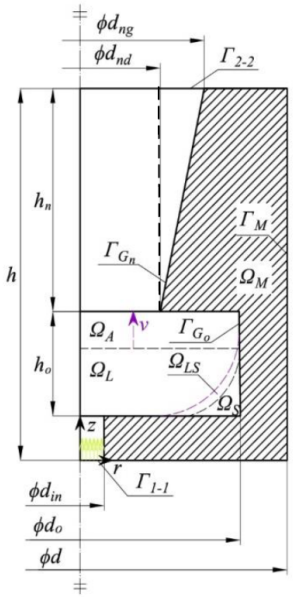

Fig. 1. Scheme and identification of sub-regions of the considered system.

The boundary conditions, specified in the considered problem, on the indicated surfaces (Fig. 1) were as follows:

— for velocity [3, 5],

$$v_t\big|_{\Gamma_{1-1}}=v_t\big|_{\Gamma_{2-2}}=v_n\big|_{\Gamma_{2-2}}=0,$$
$$v_n\big|_{\Gamma_{1-1}}=v_{in}, \qquad v_n, v_t\big|_{\Gamma_G}=0, \tag{6}$$
$$\frac{\partial v_t}{\partial n}\big|_{r=0}=0, \qquad v_n\big|_{r=0}=0,$$

— for temperature [3–6],

$$\lambda_M\frac{\partial T_M}{\partial n}\Big|_{\Gamma_M}=-\alpha_M\left(T_M\Big|_{\Gamma_M}-T_a\right),$$
$$\frac{\partial T}{\partial n}\Big|_{\Gamma_{2-2}}=0, \qquad \lambda_S\frac{\partial T_S}{\partial n}\Big|_{\Gamma_{G-}}=\lambda_G\frac{\partial T_G}{\partial n}\Big|_{\Gamma_{G-}},$$
$$\frac{\partial T}{\partial n}\Big|_{r=0}=0, \qquad \lambda_G\frac{\partial T_G}{\partial n}\Big|_{\Gamma_{G+}}=\lambda_M\frac{\partial T_M}{\partial n}\Big|_{\Gamma_{G+}},$$
$$T\,\big|_{\Gamma_{1-1}}=T_{in}, \tag{7}$$

where T_a is ambient temperature [K]; α_M — heat transfer coefficient between the ambient and the mould [W/(m^2 K)]; T_A — temperature of air inside mould cavity in initial state [K]; T_{in} — initial temperature [K]; T_M, T_G, and T_S — temperature of mould, gap (protective coating), and solid phase, respectively [K]; v_{in} — initial velocity [m/s]; λ_M, λ_S, and λ_G — thermal conductivity coefficient of mould, solid phase, and gap [W/(m K)], respectively; v_t and v_n — tangential and normal component of velocity vector [m/s], respectively; n — outward unit normal surface vector [m].

This task was solved using the finite element method (FEM) in the weighted residuals formulation [3–5].

3. Calculation results and discussion

Numerical calculations of the solidification process of the casting–riser system were made for two riser shapes, i.e., cylindrical and conical risers with the same bottom diameter. The influence of liquid metal movements on the casting solidification process in the following system of casting–riser–mould, shown schematically in Fig. 1, was also analysed.

The outside dimensions of the mould are equal to $d = 0.320$ m and $h = 0.280$ m, whereas the dimensions of the mould cavity are equal to $d_o = 0.200$ m, $h_o = 0.070$ m, $h_n = 0.150$ m, $d_{nd} = 0.080$ m, $d_{ng} = 0.100$ m, $d_{in} = 0.020$ m. For the cylindrical riser, $d_n = d_{nd} = 0.080$ m. The internal surface of the steel mould is covered with a protective coating with a thickness of 2 mm. Numerical simulations were carried out for the casting made of low-carbon cast steel and the steel mould with thermo-physical properties, which were taken from [5]. The overheated metal with the temperature of $T_{in} = 1845$ K was poured from the bottom with the velocity $v_{in} = 0.1$ m/s into the steel mould with the initial temperature $T_M = 345$ K. Other important temperatures were equal to $T_A = 345$ K and $T_a = 300$ K. The heat transfer coefficient (α) between ambient and the mould was equal to $\alpha_M = 200$ W/(m^{2}K). The professional FIDAP program was used to analyse the solidification process of the metal in the considered casting–riser system. The transient calculation process was interrupted when the temperature in the casting lowered below the solidus temperature. The computation process was carried out on a computer with a 2.3 GHz IntelCore-i7 processor and lasted approximately 24 h when using the complex model or approximately 5 h when using the basic model. Such an extension of the computation time in the first case was due to the necessity to use a very small time step in the process of filling the mould cavity.

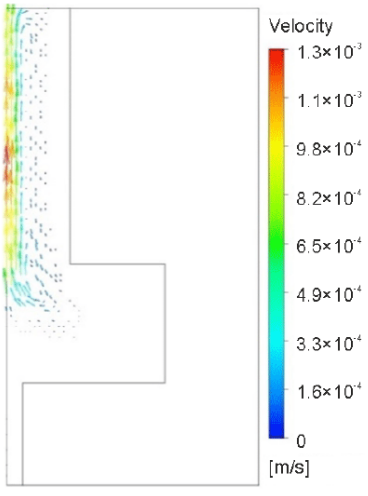

Fig. 2. Velocity vectors at $t = 400$ s, variant I.

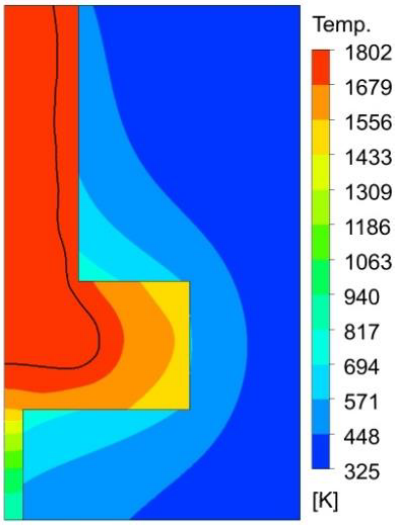

Fig. 3. Temperature distribution at $t = 400$ s, variant I.

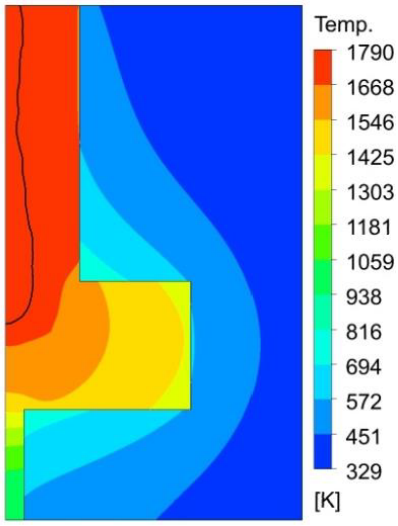

Fig. 4. Temperature field after solidification of the casting at $t = 523$ s, variant I.

Numerical calculations of the solidification process of the casting–cylindrical riser system were carried out using the complex model (variant I), while the solidification process of the casting–conical riser system was carried out using two models: complex (variant II) and basic (variant III). Simulations of the casting formation were performed, starting from the moment of filling the mould cavity with molten metal and ending with its complete solidification. Convection movements of liquid metal are presented in the form of velocity vectors for a selected moment of time (Fig. 2), while the temperature distribution corresponding to this time is shown in Fig. 3, where a solidus line is drawn separating the solid–liquid zone of the casting from its solid area.

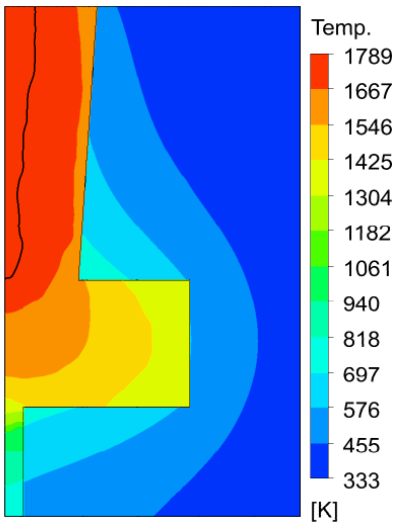

Fig. 5. Temperature field after solidification of the casting at $t = 562$ s, variant II.

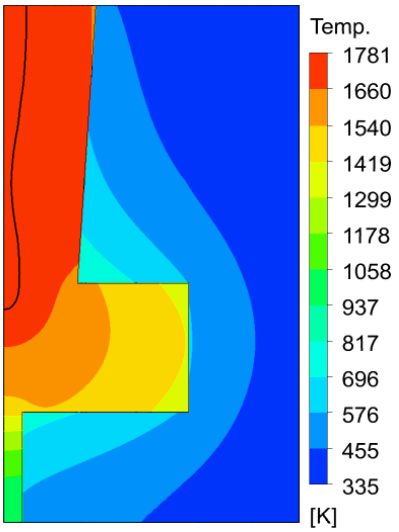

Fig. 6. Temperature field after solidification of the casting at $t = 488$ s, variant III.

Then, the temperature fields after the casting solidification for three calculation models were compared, observing the shape of the solidus line in the final stages of solidification of the casting–riser system (Figs. 4–6). When the solidus line is closed in the casting, the area limited by it will not be fed with liquid metal from the riser, and in this place, as a result of metal shrinkage, a shrinkage defect will occur (Figs. 4 and 6). However, we try to avoid such a situation and move such a defect to the riser, which can be achieved by using the complex model for calculations and the casting–conical riser system (Fig. 5).

4. Conclusions

The paper presents a mathematical model and the results of numerical simulation of the casting solidification, taking into account the process of filling the mould cavity with molten metal and convection movements after its completion (complex model), as well as simulation results in which the movements of the liquid metal were ignored (basic model). Numerical calculations of the casting solidification process were also performed for two riser shapes, i.e., cylindrical and conical riser, assumed in turn. In this way, the influence of the assumed riser shape and molten metal movements on the solidification kinetics and the location of the solidification end in the analysed system were assessed. It was observed that in the final period of solidification of the casting–riser system, a solidus line is visible closing in the upper part of the casting (in some variants). This suggests that shrinkage defects will occur at this location. This situation occurs in the case of simulation of the casting process carried out using a cylindrical riser — variant I (Fig. 4) — or when using the basic model — variant III (Fig. 6). Such a situation was not observed if the casting process was carried out using a conical riser and using a complex model — variant II (Fig. 5). In that case, the end of solidification occurred in the riser, which is desirable because the riser is cut off and reworked. It also proves that the conical-shaped riser fulfilled its task and the casting was made without casting defects, which is very important for foundry practice.

References

[1] S.L. Nimbulkar, R.S. Dalu, *Perspect. Sci.* **8**, 39 (2016).

[2] P.H. Huang, C.J. Lin, *Int. J. Adv. Manuf. Technol.* **79**, 997 (2015).

[3] R.W. Lewis, E.W. Postek, Z. Han, D.T. Gethin, *Int. J. Numer. Methods Heat & Fluid Flow.* **16**, 539 (2006).

[4] T. Skrzypczak, L. Sowa, E. Węgrzyn-Skrzypczak, *Arch. Foundry Eng.* **20**, 37 (2020).

[5] L. Sowa, T. Skrzypczak, P. Kwiatoń, *Arch. Metall. Mater.* **66**, 489 (2021).

[6] P. Kwiatoń, D. Cekus, M. Nadolski, K. Sokół, Z. Saternus, P. Pavlíček, *Acta Phys. Pol. A* **138**, 188 (2022).

[7] P.H. Huang, J.K. Kuo, T.H. Fang, W. Wu, *MATEC Web of Conf.* **185**, 00008 (2018).